KATO, N. (1974). *X-ray Diffraction*, edited by L. V. AZAROFF, ch. 4, Appendix 4A. New York: McGraw-Hill.
KATO, N., KATAGAWA, T & SAKA, T. (1971). *Kristallografiya*, **16**, 1110-1116. [Engl. transl: *Sov. Phys. Crystallogr.* (1972). **16**, 979-983. Unfortunately, the double translation causes some obscurities, so the reader is recommended to refer to the article of Kato (1974).]
PRINS, J. A. (1930). *Z. Phys.* **63**, 477-493.
ZACHARIASEN, W. H. (1945). *Theory of X-ray Diffraction in Crystals*. New York: Wiley.

*Acta Cryst.* (1992). A**48**, 834-841

# The Darwin–Prins Rocking Curve for Distorted Crystals

BY NORIO KATO

*Department of Physics, Faculty of Science and Engineering, Meijo University, Tenpaku-ku, Nagoya, Japan*

(*Received* 3 *February* 1992; *accepted* 13 *April* 1992)

## Abstract

Rocking curves (RC) of Darwin-Prins type of distorted crystals have been systematically studied with respect to various parameters which characterize the crystal and its deformation. The basic formula is given in an earlier paper [Kato (1990). *Acta Cryst.* A**46**, 672-681]. Through numerical analysis, characteristic features of RCs were deduced. In order to understand them, a simplified theory was developed based on a WKB approximation. Most of the features, in particular the oscillatory behaviour of RCs, could be interpreted by the geometrical configuration of the entrance surface and the bending *C* band, which was defined as a region where the local wave number is practically pure imaginary. The concept of the *C* band is analogous to the forbidden energy band of electrons popular in solid-state physics.

## 1. Introduction

Rocking curves (RC) in Bragg geometry are sensitive to lattice distortion near the crystal surface. Taupin (1964) proposed a fundamental (differential) equation to calculate the intensity of the Bragg reflection for distorted crystals. Since then, the theory has been widely used in many investigations. For example, Burgeat & Taupin (1968) and Fukuhara & Takano (1977) studied experimental RCs of impurity-doped crystals and showed a reasonable agreement with the theoretical curve based on the erfc-function model for the lattice distortion. More recently, Bensoussan, Malgrange & Sauvage-Simkin (1987) presented a similar work for a III-IV* heterojunction system. Many relevant articles are cited in that paper. They also obtained a good agreement between Taupin's theory and their experimental results. It seems, therefore, that there remains no serious problem in this research field from the practical point of view.

All authors, however, solve Taupin's differential equation numerically assuming some plausible model for the lattice distortion depending on their own samples. For this reason, it seems desirable to make a systematic analysis of RCs based on an exact and analytical solution of the wave field, which has been obtained recently by the present author (Kato, 1990). This is the primary subject of the present paper.

Here, the lattice spacing is assumed to have the form $D_o \tanh(\alpha x)$, where $x$ is the coordinate normal to the net plane concerned. The model is similar to that of Bensoussan *et al.* (1987). By changing $D_o$, $\alpha$ and the position of the entrance surface $x_e$, one can represent various monotonic forms of the lattice expansion effective for diffraction. These forms give rise to different shapes of RC. There are parameters of another type characterizing the crystal concerned, which also change the shape of the RC. They are the structure factor and the normal and Borrmann absorption. With this complex situation in mind, results will be presented in terms of suitably normalized parameters (§ 3).

One interesting phenomenon is the oscillatory behaviour of a RC which appears under specific conditions. The phenomenon itself was recognized in both numerical simulations and real experiments by the authors mentioned above. Here, characteristic properties are interpreted by a simple theory to elucidate the physical significance (§ 4).

## 2. Glossary of formulae and parameters

### (*a*) *Perfect crystals*

In order to give an idea of the present scheme of notation, RCs of perfect crystals are first dealt with. We are concerned only with the symmetrical case. The theoretical details are described in standard texts

* Groups 13-14 in IUPAC (1988) nomenclature.

0108-7673/92/060834-08$06.00

on dynamical diffraction, for example those of Zachariasen (1945), James (1962), Batterman & Cole (1964) and Kato (1974). Also, the previous paper by the present author (Kato, 1992) is referred to. Following this subsection, a summary for distorted crystals will be presented.

(i) *Vacuum waves.*

Incident wave:

$$D_e \exp(i\mathbf{K}_e\cdot\mathbf{r}); \tag{2.1a}$$

diffracted wave:

$$D_g \exp(i\mathbf{K}_g\cdot\mathbf{r}) \tag{2.1b}$$

where

$$\mathbf{K}_e = \bar{\mathbf{K}}_o - \Delta\mathbf{K}_o \tag{2.2a}$$

$$\mathbf{K}_g = \bar{\mathbf{K}}_g - \Delta\mathbf{K}_g. \tag{2.2b}$$

$\bar{\mathbf{K}}_o$ and $\bar{\mathbf{K}}_g = \bar{\mathbf{K}}_o + 2\pi\bar{\mathbf{g}}$ are the wave vectors satisfying the Bragg condition exactly in a kinematical sense, $\bar{\mathbf{g}}$ being the reflection vector. $\Delta\mathbf{K}_o$ and $\Delta\mathbf{K}_g$ indicate the deviation of the wave vectors from the exact Bragg condition.

We shall take a system of rectangular axes which are tangential (**t**) and outwardly normal (**x**) to the crystal surface, respectively, within a plane defined by $\bar{\mathbf{K}}_o$ and $\bar{\mathbf{K}}_g$. The third axis will be suppressed.

The components of any vector **A** defined in real or reciprocal space are denoted in parentheses as $(A_t, A_x)$. With this convention, the vectors in (2.1) and (2.2) are specified as follows.

Position vector:

$$\mathbf{r} = (t, x). \tag{2.3}$$

Wave vector:

$$\bar{\mathbf{K}}_o = K(\cos\theta_B, -\sin\theta_B) \tag{2.4a}$$

$$\bar{\mathbf{K}}_g = K(\cos\theta_B, \sin\theta_B) \tag{2.4b}$$

$$\Delta\mathbf{K}_o = (E, E/c), \quad \Delta\mathbf{K}_g = (E, -E/c) \tag{2.5a,b}$$

$$E = K\sin\theta_B\Delta\theta \tag{2.6}$$

$$c = \tan\theta_B. \tag{2.7}$$

In these expressions, $\theta_B$ is the exact Bragg angle and $\Delta\theta$ is the angular deviation of $\mathbf{K}_e$ from $\bar{\mathbf{K}}_o$.

(ii) *Crystal waves.*

*O* wave:

$$d_o \exp(i\mathbf{k}_o\cdot\mathbf{r}); \tag{2.8}$$

*G* wave:

$$d_g \exp(i\mathbf{k}_g\cdot\mathbf{r}) \tag{2.9}$$

where

$$\mathbf{k}_o = \bar{\mathbf{K}}_o - \Delta\mathbf{k}, \quad \mathbf{k}_g = \bar{\mathbf{K}}_g - \Delta\mathbf{k} \tag{2.10a,b}$$

$$\Delta\mathbf{k}\text{: } (E, [\varepsilon^2 - M^2]^{1/2}/c). \tag{2.11}$$

The phase angle of $[\ldots]^{1/2}$ in the complex plane is fixed between 0 and $\pi$. The other parameters are defined as follows.

$$\varepsilon = E - (1/2)\tau_c + (i/2)\mu_c \tag{2.12}$$

$$\tau_c = K(-\chi_o')/\cos\theta_B \quad (\geq 0) \tag{2.13a}$$

$$\mu_c = K(\chi_o'')/\cos\theta_B \quad (\geq 0) \tag{2.13b}$$

$$M = \tfrac{1}{2}KP(\chi_g\chi_{-g})^{1/2}/\cos\theta_B \tag{2.14a}$$

$$= M_o \exp(i\Phi/2) \tag{2.14b}$$

$$M_o = \tfrac{1}{2}KP(\text{abs}\,[\chi_g\chi_{-g}])^{1/2}/\cos\theta_B \tag{2.14c}$$†

$$\Phi = \arg[\chi_g\chi_{-g}]. \tag{2.14d}$$

In these expressions, $P$ is the polarization factor and $\chi_o$, $\chi_g$ and $\chi_{-g}$ *etc.* are the Fourier coefficients of the complex polarizability ($\chi = \chi' + i\chi''$) of the crystal, so that $M$ is complex in general. The imaginary part of $\chi_g\chi_{-g}$ gives rise to Borrmann effects. In the definition of $\chi$, the polarizability defined in electromagnetic theory is multiplied by $4\pi$.

(iii) *The amplitude ratio and reflectivity.*

$$C_g = D_g/D_o = (\chi_g/\chi_{-g})^{1/2}M^{-1}\{-\varepsilon + [\varepsilon^2 - M^2]^{1/2}\} \tag{2.15}$$

Reflectivity:

$$R = |C_g|^2. \tag{2.16}$$

### (*b*) *Distorted crystals*

Here the relevant results of a previous paper (Kato, 1990) are summarized. [*P.*] indicates the equation number in that paper. A few modifications are made in order to extend the applicability to the case including Borrmann absorption. * indicates modified formulae.

Often, the following variables are used to specify a position instead of the coordinate $x$:

$$\xi = \tanh\alpha x \quad [\alpha > 0] \tag{2.17a}$$

$$z = (1+\xi)/2. \tag{2.17b}$$

Also, the subscript $e$ is attached to them to denote the position on the entrance surface.

(i) *The lattice distortion.* We are concerned with the distorted crystal, in which the $x$ component of the reflection vector is given in the form

$$g(x) = \bar{g} - (1/\pi c)D_o\tanh(\alpha x). \tag{2.18}$$

[*P.*3.2, *P.*3.3]

In other words, the assumed lattice expands along the $x$ direction. The lattice is perfect in the regions

† In this paper, for generality, $M_o$ is defined as proportional to $(\text{abs}\,[\chi_g\chi_g])^{1/2}$ instead of the traditional definition using $|\chi_g'|$ (see Kato, 1992).

with $x=\pm\infty$ but has different spacings. Henceforth, nearly perfect regions for a sufficiently large $\pm\alpha|x|$ are called top-perfect region (TPR) and bottom-perfect region (BPR), respectively. Also, the region with $\alpha|x|\leq 1$ is called the transient region (TR). Notice that the crystal in the region with $x>x_e$ is virtual.

The following parameters are introduced for hypergeometric functions which will appear soon.

$$\bar{\nu}=D_o/\alpha c \qquad [P.4.2a] \qquad (2.19)$$

$$p+q=-i[(\varepsilon-D_o)^2-M^2]^{1/2}/\alpha c \qquad [P.4.7a] \qquad (2.20a)$$

$$p-q=-i[(\varepsilon+D_o)^2-M^2]^{1/2}/\alpha c \qquad [P.4.7b] \qquad (2.20b)$$

$$a=-i\bar{\nu}+q, \quad b=1+i\bar{\nu}+q, \quad c'=1+q+p. \qquad [P.4.12a,b,c] \qquad (2.21a,b,c)\dagger$$

Here, the standard notation $c$ is replaced by $c'$ to avoid any confusion with $c$ defined by (2.7).

(ii) *The vacuum waves.* The same expressions as in (2.1$a$,$b$) are used for the incident and Bragg-reflected waves. Notice, however, that $\bar{g}$ is defined at $x=0$.

(iii) *Reflectivity.* The rocking curve of Darwin-Prins type is given in the form

$$R=|C_a|^2\times\left|\frac{F[i\bar{\nu}+q,1-i\bar{\nu}+q;1+p+q;(1+\xi_e)/2]}{F[-i\bar{\nu}+q,1+i\bar{\nu}+q;1+p+q;(1+\xi_e)/2]}\right|^2 \qquad [P.5.6b] \qquad (2.22)$$

where

$$C_a=-M_g^{-1}(\alpha c/\bar{\nu})(i\bar{\nu}-p)(i\bar{\nu}-q) \qquad [P.4.16b];\ [P.4.17]^* \qquad (2.23a)$$

$$=(\chi_g/\chi_{-g})^{1/2}M^{-1}\{[(\varepsilon-D_o)^2-M^2]^{1/2}-(\varepsilon-D_o)\}. \qquad [P.5.7]^* \qquad (2.23b)$$

Comparison of (2.23$b$) with the expression for $C_g$ [(2.15)] indicates that $|C_a|^2$ is the reflectivity of the perfect crystal corresponding to BPR. The second factor of (2.22) is intrinsic to the lattice distortion.

Before closing this glossary, it is worthwhile mentioning the normalization of equations. For this purpose, we shall introduce three characteristic distances:

$$\Lambda=cM_o^{-1}\text{: a kind of extinction distance} \qquad (2.24a)$$

$$\Lambda_a=\mu_c^{-1}\text{: a measure of absorption distance} \qquad (2.24b)$$

$$\Lambda_d=\alpha^{-1}\text{: a measure of the thickness of the TR.} \qquad (2.24c)$$

Then, the formulae listed above can be rewritten in normalized forms with the use of the dimensionless quantities

$$X=x/\Lambda \qquad (2.25a)$$

$$A=\Lambda/\Lambda_a \qquad (2.25b)$$

$$H=M_o/\alpha c=\Lambda_d/\Lambda \qquad (2.25c)$$

and other ones such as $\tilde{D}_o=D_o/M_o$ and $\tilde{\varepsilon}=\varepsilon/M_o$. For example, (2.20) can be written in the form

$$p\pm q=-i[(\tilde{\varepsilon}-\tilde{D}_o)^2-\exp i\Phi]^{1/2}H. \qquad (2.26)$$

The normalized formulae are useful not only for considering the theoretical structure of RCs but also for numerical calculation. Nevertheless, since the transformation is a matter of simple algebraic manipulation, we shall not write them repeatedly.

## 3. Numerical results

In the present treatment, the lattice distortion is described primarily by two parameters, $D_o$ and $\alpha$ [(2.18)] or $H$ [(2.25$c$)]. Since, however, the distortion is defined in absolute space, the position of the entrance surface $x_e$ (or $z_e$) is an essential parameter which specifies the lattice distortion concerned. Moreover, since crystals usable for diffraction are limited by the absorption distance $\Lambda_a$, it is also an implicit parameter for the effective distortion.

Because RCs depend on many parameters, the following description will be divided into four subsections with the use of the normalized parameters defined by (2.24) and (2.25). First, the dependence of $X_e$ is described for $A<0.1$ and $H=1$. However, non-absorbing cases are separately described since the behaviour is singular in a sense. Next, the dependence on absorption is described for fixed $X_e$ and $H$. In the third subsection, $H$ dependence for fixed $X_e$ and $A$ is dealt with. Up to this subsection, for simplicity, the phase angle $\Phi$ in (2.14$b$) is assumed to be zero. The behaviour for a finite $\Phi$ (the effect of Borrmann absorption) is given in the fourth subsection. In the final subsection, some remarks on the computation will be mentioned.

In all illustrations, for the sake of completeness, $D_o/M_o$ is fixed to be 3 and $\alpha$ is assumed to be positive. Therefore, the Bragg reflections corresponding to TPR and BPR will appear, if they exist, with centres at $E/M_o=-3$ and 3, respectively. The opposite sign assignment to $\alpha$ leads to similar conclusions on the opposite side of the $E/M_o$ axis.

### (*a*) *The dependence on the position* $X_e$ ($H=1$)

(i) *Non-absorbing crystals.* This case has been discussed analytically in a previous paper. Some numeri-

† Since we are concerned with the solution of type $a$ defined in the previous paper, which is regular in the BPR, $p$ is replaced by $-p$. The same is applied to the sign of $\xi$ in (2.17$b$). See [*P.*4.13$b$].

cal results are illustrated in Figs. 1($a$) and ($b$). The total reflection always appears in the angular range ($4 \geq E/M_o \geq 2$), which is that expected for a perfect crystal corresponding to BPR. The physical reason for this was discussed by Kato (1990). In neutron experiments, therefore, the appearance of total reflection is not necessarily an indication of perfectness near the crystal surface.

When the entrance surface locates inside the TR with a negative $X_e$, only a slight enhancement is detectable on the low-angle side of the total reflection. If $X_e$ is positive, the enhancement is intensified. When the entrance surface is far above the TR ($X_e/H > 3.5$), another enhanced reflection appears in an angular range near ($-2 \geq E/M_o \geq -4$). In the extreme case where $X_e$ is sufficiently large, it tends to have a top-hat shape [see (vi) of Fig. 1($b$)], which is the Bragg reflection corresponding to the TPR.

More important is that oscillatory behaviour is expected in the angular range between the two Bragg reflections. This is characteristic when the TR lies below the crystal surface. This subject will be discussed in § 4. In experiments in which only one oscillation peak appears [(iv) of Fig. 1($b$)], it must not be misunderstood as the Bragg reflection corresponding to the TPR.

(ii) *Small-absorption crystals* ($c\mu_c/M_o = A \cong 0.1$). When the parameter $X_e$ is large and negative, the RC is not so characteristic. Total reflection is no longer expected. The behaviour of a weakly absorbing perfect crystal corresponding to the BPR is nearly preserved.

Fig. 2 illustrates a few examples of RCs for the same values of $X_e$ and $H$ used in Fig. 1. If $X_e$ is nearly equal to zero, the Bragg reflection due to the BPR takes an asymmetric form and the tail on the low-angle side is enhanced. When $X_e$ increases positively, another reflection peak corresponding to the TPR appears, as easily anticipated. Again, more significant is that the tail on the high-angle side of this peak shows an oscillation. The number of oscillations increases almost proportionally to $X_e$. Table 1 shows the number for different values of $X_e$. We notice also that the angular range of the oscillation is limited within $D_o + M_o \geq E \geq M_o - D_o$ ($4 \geq E/M_o \geq -2$ in our numerical model).

### ($b$) *The dependence on absorption*

Fig. 3 is the contour plot of the reflectivity $R$ projected on the $A$, $E/M_o$ plane. Any section with a fixed $A$ represents a rocking curve. In this figure, $H = 2$ and $X_e = 4.60$ ($\xi_e = 0.98$) are fixed.

As mentioned in § 3($a$)(i), the non-absorbing case (the base line) is singularly different from that of finite absorption. The thick line indicates the angular range of the total reflection. Except for this special case, one can see oscillatory behaviour in the angular range $4 > E/M_o > -2$. The peak positions are almost unaltered by the absorption parameter $A$ although the intensity decreases as $A$ increases.

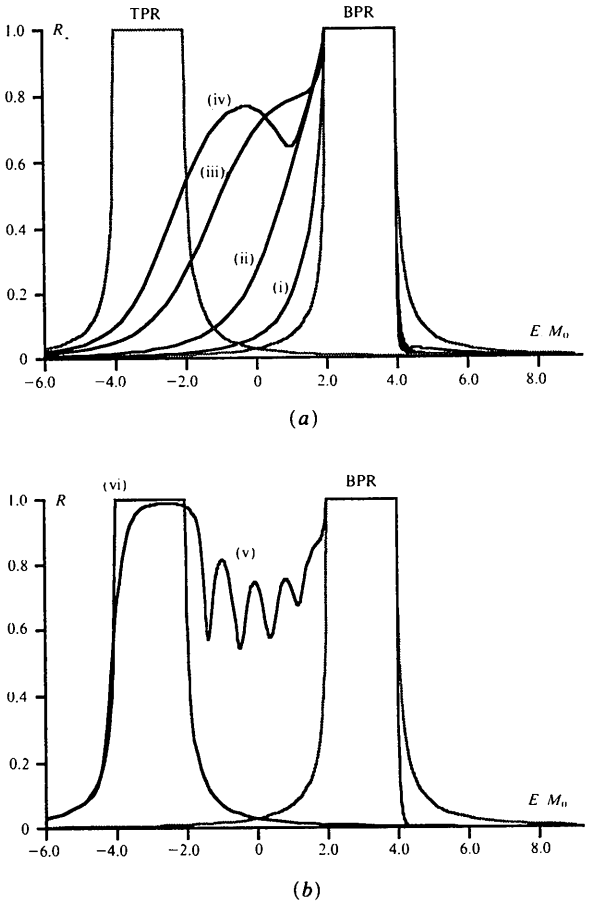


Fig. 1. Rocking curves of distorted crystals under the conditions $A = 0$ and $H = 1$. The label of each curve indicates the position of the entrance surface: (i), (ii), (iii), (iv) (v), (vi) correspond to $\xi_e = \{-0.6, 0.0, 0.6, 0.8, 0.998, 1\}$, *i.e.* $X_e = \{-0.69, 0.0, 0.69, 1.10, 3.45, \infty\}$. Curves indicating RCs of perfect crystals corresponding to BPR and TPR are also shown.

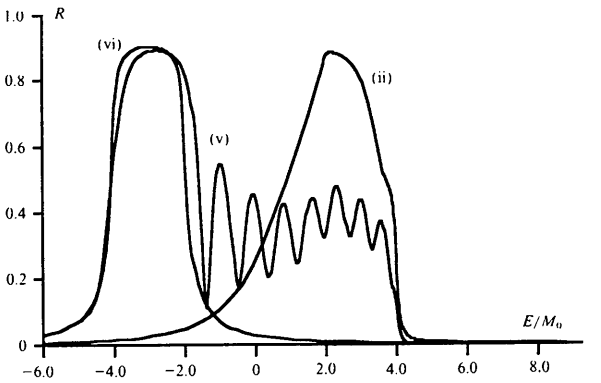


Fig. 2. Rocking curves of distorted crystals under the conditions $A = 0.1$ and $H = 1$. The labels have the same meaning as in Fig. 1.

### (c) *The dependence on H*

In § 3(*a*), we discussed the case with $H = \Lambda_d/\Lambda = 1$. If either the distortion is gentle or the structure factor is large, it may occur that the TR is much thicker than the extinction distance, *i.e.* $H \gg 1$. The reverse case is also conceivable. It is a general rule that the strain gradient times the extinction distance is a key parameter in diffraction phenomena of distorted crystals (Kato, 1964). For a fixed $D_o$, $H^{-1}$ is the key parameter for the present problem in this sense.

It should be noticed that the parameters $p$, $q$ and $\bar{\nu}$ which determine the reflectivity are linear with respect to $H$ [(2.19), (2.20) and (2.26)]. This implies that the factor $C_a$ is $H$ independent and the $H$ dependence of the RC comes from the second factor which includes hypergeometric functions. There, not only the linear dependence of $p$, $q$ and $\bar{\nu}$ but also the $H$ dependence of $z_e = \frac{1}{2}[1+\tanh(X_e/H)]$ must be kept in mind.

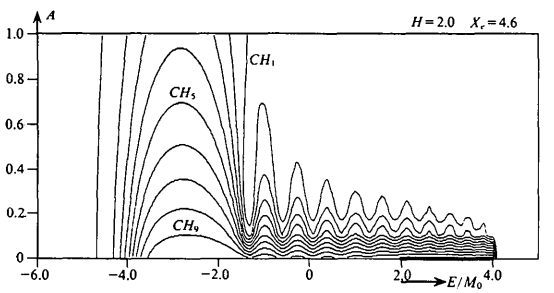


Fig. 3. The contours of the reflectivity projected on the $A, E/M_o$ plane ($H = 2$, $X_e = 4.6$).

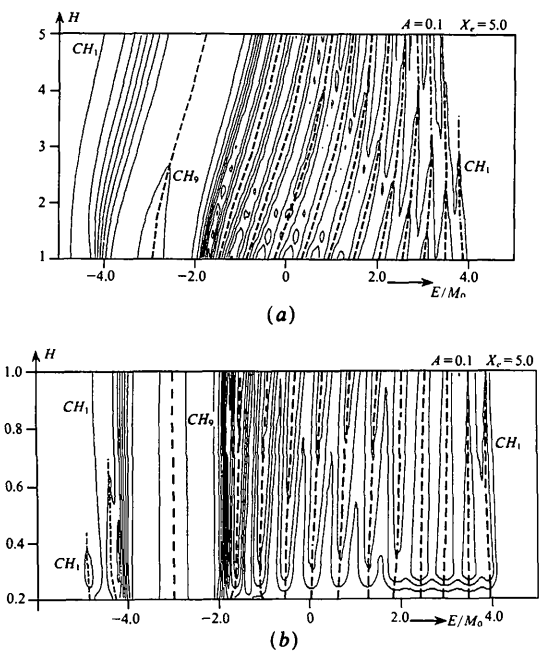


Fig. 4. The contours of the reflectivity projected on the $H$, $E/M_o$ plane ($A = 0.1$, $X_e = 5.0$). $CH_m$ indicates the height of contours, which is $m$ times the unit of increment, 0.1. (*a*) $H \geq 1$. (*b*) $H \leq 1$.

Table 1. *The number of fine peaks of RCs* ($A = 0.1$)

| $X_e$ | $H = 0.5$ | $H = 1$ | $H = 2$ |
|---|---|---|---|
| 1 | 2 (0.5) | 2 (2.8) | 3 (3.9) |
| 2 | 4 (4.7) | 4 (4.9) | 5 (5.7) |
| 3 | 6 (6.9) | 6 (7.1) | 7 (7.8) |
| 4 | 9 (9.1) | 9 (9.3) | 9 (9.9) |
| 5 | 11 (11.3) | 11 (11.5) | 11 (12.1) |

Integers given beneath $H$ are the number calculated by the exact formula (2.22) and the figures in parentheses are the numbers estimated by the simple theory described in § 4.

If $H \gg |X|$, the $D$ field [$D(X) = D_o \tanh(X/H) + E$, omitting absorption] is practically reduced to $D = E$. If the crystal surface is located in this region, the Bragg reflection occurs near $E = 0$. When $H \ll |X|$, again, the $D$ field is independent of $X$ but splits into $D = E \pm D_o$ depending on the sign of $X$. If $X_e$ lies in this region, the Bragg peak is expected at $E = -D_o$ or $+D_o$. In this case, the TR is practically parallel to the entrance surface. The model of lattice distortion represents a superposition of two perfect crystals if $X_e$ is positive. If it is negative, the whole crystal is nearly perfect so that the case is trivial in our problem.

These general remarks will be useful for considering the following examples.

(i) *The cases of* $H > 1$ (*gentle distortion*). Fig. 4(*a*) illustrates the contours of the reflectivity for $X_e = 5.0$ and $A = 0.1$. For increasing $H$, the main Bragg peak shifts towards $E = 0$ because of the $H$ dependence of $z_e$. Accordingly, the oscillatory peaks also shift to the large-angle side. Nevertheless, the number of peaks is not changed. It is worth noting that the number of oscillations is determined by $X_e$. The number is practically independent of $H$ as shown in Table 1.

Another characteristic feature is that the upper range of $E/M_o$ where the oscillation occurs is limited by $D_c + M_o$ (=4 in our model). As will be discussed in § 4, this is a key to understanding the oscillation phenomena.

(ii) *The case of* $H < 1$ (*steep distortion*). Fig. 4(*b*) illustrates similar contours for the same values of $A$ and $X_e$ as in Fig. 4(*a*). In this case, $\xi_e$ is more than 0.999 for $X_e = 5$. This implies that the main Bragg reflection always appears near the angular position corresponding to TPR. The oscillatory peaks are nearly parallel to the $H$ axis.

For $H < 0.4$, one can see a few fine peaks also in the angular regions outside $-(D_o + M_o)$ and $(D_o + M_o)$. It is also significant that all oscillations disappear when $H < \sim 0.2$. In order to show clearly these exceptional properties for steep distortions, the RCs for $H = 0.3$ and 0.2 (dashed curve) are illustrated in Fig. 5(*a*). The physical reasons will be discussed in § 4.

### (*d*) *Effects of Borrmann absorption*

So far, for simplicity, we have assumed that $\Phi = 0$. In this section, we discuss the case in which $\Phi$ is finite. Usually, however, $|\tan \Phi|$ is less than unity. It is also worth bearing in mind that the maximum of $|\sin(\Phi/2)|$ is limited by $A/2$ to satisfy the physically allowable condition $|\chi_0^i| \geq |\chi_g^i|$. In perfect crystals, this limiting case gives a total reflection singularly at the right or left edge of the Bragg peak depending on the sign of $\Phi$ (*cf.* Zachariasen, 1945; Kato, 1992).

Fig. 5(*b*) shows RCs for the negative limiting value of $\Phi$ and the same values of other parameters used in Fig. 5(*a*). We notice that the main features of the RC are not much different from those for $\Phi = 0$. In particular, the angular positions of the fine peaks are nearly identical. Again, in the case of $H = 0.2$ (the broken curve), all oscillations of RC disappear.

The main Bragg peak is different from that for $\Phi = 0$, but very similar to the RC expected for perfect crystals. In the present numerical model, the singular peak is expected to be at the angular position where $E/M_o = -4$.

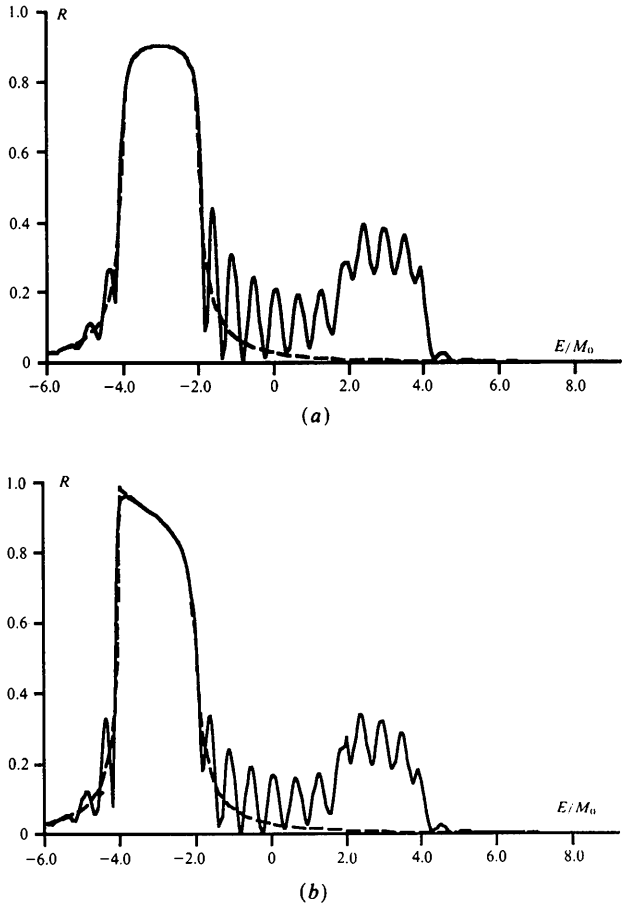


Fig. 5. Examples of RCs for small $H$ ($A = 0.1$, $X_e = 5.0$). The full curve corresponds to $H = 0.3$. The dashed curve corresponds to $H = 0.2$. (*a*) $\Phi = 0$. (*b*) $\sin(\Phi/2) = -A/2 = -0.05$.

### (*e*) *Technical problems in the computation*

The present task depends entirely on how to calculate the hypergeometric functions of complex arguments in (2.22). Owing to recent advances in computer technology, such transcendental functions are easily calculated even on the personal-computer level. Also, graphic software programs can give a global view of the function concerned. Most RCs presented above, which consisted of more than 100 points of reflectivity, could be obtained in about 10 min or less.

Mathematically, the hypergeometric functions concerned are undefined when the argument $c'$ [(2.21*c*)] takes negative integers (see, for example, Abramowitz & Stegun, 1964, p. 556), although the ratio to give the reflectivity is finite as it should be. Also, since each function is singular at $\xi_e = 1$, it was thought at the beginning that computing a RC in that case would bring about a problem. In practice, however, no trouble occurred with commercial applications. Strikingly, at least to the author, the curve TPR of Fig. 1(*a*) and curve (vi) of Fig. 1(*b*) were identical. Incidentally, the former was calculated by the classical Darwin formula (2.15) with the use of $E + D_o$ for $E$ and the latter was obtained by (2.22).* Thus, all physical cases such as perfect and distorted crystals, non-absorbing and highly absorbing crystals and thick crystals could be dealt with by the single formula (2.22).

## 4. A simple interpretation of the oscillation in RCs

Since the wave function $u$ as well as $v$ [*P*.2.9] obeys an ordinary differential equation, its approximate solution is obtainable by a kind of WKB method provided that the distortion is gentle. (*cf.*, for example, Jeffreys & Jeffreys, 1956). In this section we shall see how far such an approximate solution can describe the oscillatory behaviour of RCs described in § 3.

For this purpose, the local wave number $\Delta k$† defined by

$$i\Delta k = \mathrm{d}/\mathrm{d}x(\log u) \qquad (4.1)$$

is investigated. Then, we shall have an equation of Riccati type for $\Delta k$,

$$(\Delta k)^2 - i(\Delta k)' = c^{-2}(D^2 + icD' - M^2) \qquad (4.2)$$

where the deviation field $D$ is defined by

$$D(x) = E + i\mu_c/2 + D_o \tanh(\alpha x). \quad [P.2.10] \qquad (4.3)$$

Here, assuming a moderately weak distortion, we neglect the derivatives $\Delta k'$ and $D'$ in (4.2). Also, we assume weak absorption so that $M$ is replaced by $M_o$

* It is true, as proved analytically in a previous paper (Kato, 1990), that they must be identical if an (artificial) infinitesimal absorption is introduced.

† From the viewpoint of the solution of the original Maxwell equation, $\Delta k$ is the deviation from the global wave vector $\bar{\mathbf{K}}_o$ or $\bar{\mathbf{K}}_g$.

and $\mu_c$ is neglected in (4.3). Physically, however, a weak damping of waves is to be kept. Otherwise, the behaviour of the RC would be singular.

Under these approximations, the traces of $\Delta k = 0$ are given by the two contours in $E,x$ space,

$$E + D_o \tanh(\alpha x) = \pm M_o. \tag{4.4}$$

They are denoted by $C1$ and $C2$ in Fig. 6. The area enclosed between them is henceforth called the $C$ band.

Outside and inside the $C$ band, $\Delta k$ is purely real and imaginary, respectively, and takes twofold values,

$$\Delta k_\pm = \pm c^{-1}(D^2 - M_o^2)^{1/2}. \tag{4.5}$$

Thus, one may construct an approximate wave function $u$ by a linear combination of two independent solutions in the form

$$u(x) = c_1 u_+(x) \exp\left[i \int_{x_c}^{x} \Delta k_+ \, dx\right] + c_2 u_-(x) \exp\left[i \int_{x_c}^{x} \Delta k_- \, dx\right] \tag{4.6}$$

where $c_1$ and $c_2$ are numerical constants, $u_+$ and $u_-$ are amplitudes and $x_c$ is an arbitrary position at this stage. A similar expression is obtained for $v(x)$.

Next, we shall seek a special solution in each domain of $E,x$ space, which meets the boundary conditions for a half-infinite crystal. The deviation parameter $E$ is specified by a point on one of the three segments $E_r$, $E_i$ and $E_m$, which are divided by $C1$ and $C2$ and the vertical line $V2$ at $E = 4$ in Fig. 6. If the position of the entrance surface $x_e/\Lambda$ is less than around $-H$, the segment $E_m$ is practically negligible.

If $E$ belongs to the segment $E_r$, the crystal wave excited on the entrance surface must propagate along the $-x$ direction (downwards) throughout the crystal. Therefore, only the second term on the right of (4.6) is to be selected. Similarly, only the second term is allowable when $E$ belongs to the segment $E_i$ because the crystal wave must attenuate downwards. In this case a large Bragg reflection is expected. In any case we have no reason to expect the oscillation of RC.

When $E$ belongs to the segment $E_m$, the crystal wave between the entrance surface and the contour $C2$ consists of the two terms in (4.6) because the wave propagating downwards is reflected near $C2$. Here, we shall put the postulation

$$u(x_c) = v(x_c) = 0 \tag{4.7}$$

after fixing $x_c$ on $C2$. This implies that the crystal wave is totally reflected and no wave propagates inside the $C$ band. Under this postulation, the interference term (ITR) of the reflectivity has the form

$$\mathrm{ITR} = V \cos\left[2c^{-1} \int_{x_c}^{x_e} (D^2 - M_o^2)^{1/2} \, dx\right] \tag{4.8}$$

where $V$ is a slowly varying function of $x_c$ related to $v_\pm$, which is regarded as a constant in the following arguments. Since $D$ and $x_c$ depend on the deviation parameter $E$, one can expect the oscillation of the RC in the range of the segment $E_m$.

Here, we are concerned specifically with the total number $N$ of oscillations of the RC. From (4.3) and (4.8), $N$ is given by

$$N = \pi^{-1} \int_{x_c}^{x_e} \{[\tilde{E}_o + \tilde{D}_o \tanh(X/H)]^2 - 1\}^{1/2} \, dX \tag{4.9}$$

where the normalized parameters are used to conform with the convention used in § 3 and $X_c$ and $\tilde{E}_o$ are the values at the right end of $E_m$; namely, $\tilde{E}_o = \tilde{D}_o + 1 = 4$ and $X_c$ is $-\infty$. Integrating (4.9) numerically with these values, one can obtain $N$. Some results are shown in Table 1. The agreement with the values obtained through RCs calculated by the exact expression (2.22) is reasonable.

It is clear that the oscillation does not appear when $E$ belongs to the segment $E_r$; *i.e.* outside the vertical lines $V1$ and $V2$ in Fig. 6 as well as in the case that $X_e < \sim -H$. These are general rules for gentle deformations as described in § 3. However, one cannot interpret straightforwardly a few peaks outside $V1$ and $V2$ mentioned in § 3(*c*)(ii). This is unavoidable because the WKB approximation may break down for a steep deformation particularly near the contours $C1$ and $C2$. Similarly, the fact that the oscillations disappear for $H$ less than 0.2 is not explained directly by the simple theory. Physically, however, it can be anticipated because then a kind of tunnelling of the waves may occur through the $C$ band. In fact, the $C$ band becomes thinner and thinner with decreasing $H$.

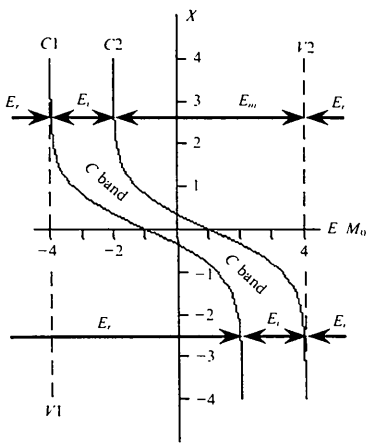


Fig. 6. The geometrical configuration of the entrance surface and the $C$ band. The two thick lines with arrows indicate the typical positions of the entrance surface (see § 4 on the notations $E_r$, $E_i$ and $E_m$).

## 5. Discussion

The reflectivity of the Bragg reflection for the specific lattice expansion described in the *Introduction* can be given by (2.22). Although the expression itself is simple, the hypergeometric function involved is not very popular. For this reason, results of RCs for typical cases were shown. In § 3, RCs and contour plots of the reflectivity were illustrated for various parameters. Through this task, characteristic features of RCs could be deduced.

In order to understand RCs a simple theory based on the WKB approximation was developed in § 4. In general, both $O$ and $G$ waves can be represented in terms of two exponential functions [*cf.* (4.6)] replacing the hypergeometric function in the exact theory. A useful concept is the $C$ band in $x,E$ space, which was defined as a region where the local wave number is purely imaginary. Most of the features described in § 3 can be interpreted by the geometrical configuration of the $C$ band with respect to the entrance surface, its form depending on the width $H$ of the deformed region.

The oscillation of RCs occurs only when the bending $C$ band (*i.e.* the TR) lies below the crystal surface. The $C$ band plays a role analogous to the forbidden energy band of electrons in a solid. It reflects the crystal wave because propagating waves cannot exist in it. The oscillation of RCs is due to the interference of two waves propagating downwards and upwards in the crystal in the manner of waves in a slab crystal. The number of oscillations estimated by the simplified theory agrees well with that obtained by the exact theory.

If the entrance surface simply cuts the $C$ band, a large Bragg peak is expected. Notice that the angular width of this peak is nearly the same as that of the perfect crystal. This is understandable because the width of $E_i$ is always $2M_0$ as shown in Fig. 6. If there exists no $C$ band below the crystal surface, the crystal wave only propagates downwards so that the oscillation is not expected. These principles will be widely applicable to other forms of lattice distortion.

As mentioned in the previous paper, the original theory is also applicable to a wide variety of distortion, provided that the distortion is of a monotonic and stratified type. If one remembers the simple relation

$$[(1-F)\exp(\alpha x)-(1+F)\exp(-\alpha x)] \times[\exp(\alpha x)+\exp(-\alpha x)]^{-1} = \tanh(\alpha x)-F \quad (5.1)$$

and notices that the constant $F$ can be absorbed into the deviation parameter $E$ in the $D$ field, [*P*.2.10], [*P*.4.2], (2.22) can be used with some modifications of the relevant parameters. Obviously, the present theory corresponds to $F=0$ and the deformation assumed by Bensoussan *et al.* (1987) corresponds to $F=-1$. Therefore, the present theory could be used also in their case.

Experimentally, the oscillation number can be used to estimate the depth of a heterojunction of two crystals or the boundary of an impurity-doped region below the crystal surface. Also, the pitch of the oscillation can be used as a measure of the angular resolution in diffraction apparatuses which need a subsecond resolution.

As shown in Fig. 5, one may not detect the oscillation even with a sufficiently high-resolution power in angle. Such a negative observation, however, is a good indication of small $H$, namely a sharp junction of two crystals having different lattice spacing.

### References


ABRAMOWITZ, M. & STEGUN, I. A. (1964). *Handbook of Mathematical Functions.* National Bureau of Standards, United States Department of Commerce, Washington, DC, USA.

BATTERMAN, B. W. & COLE, H. (1964). *Rev. Mod. Phys.* **36**, 681-717.

BENSOUSSAN, S., MALGRANGE, C. & SAUVAGE-SIMKIN, M. (1987). *J. Appl. Cryst.* **20**, 222-229.

BURGEAT, J. & TAUPIN, D. (1968). *Acta Cryst.* A**24**, 99-102.

FUKUHARA, A. & TAKANO, Y. (1977). *Acta Cryst.* A**33**, 137-142.

JAMES, W. (1962). *Solid State Physics*, edited by F. SEITZ & D. TURNBULL, Vol. 15, pp. 53-220. New York: Academic Press.

JEFFREYS, H. & JEFFREYS, B. S. (1956). *Methods of Mathematical Physics*, p. 522. Cambridge Univ. Press.

KATO, N. (1964). *J. Phys. Soc. Jpn*, **19**, 67-77.

KATO, N. (1974). *X-ray Diffraction*, edited by L. V. AZAROFF, ch. 4. New York: McGraw-Hill.

KATO, N. (1990). *Acta Cryst.* A**46**, 672-681.

KATO, N. (1992). *Acta Cryst.* A**48**, 829-834.

TAUPIN, D. (1964). *Bull. Soc. Fr. Minéral. Cristallogr.* **87**, 469-511.

ZACHARIASEN, W. H. (1945). *The Theory of X-ray Diffraction in Crystals.* New York: Wiley.